Author Manuscript

Author Manuscript

Author Manuscript

Author Manuscript

HHS Public Access

Author manuscript

Curr Alzheimer Res. Author manuscript; available in PMC 2019 February 06.

Published in final edited form as:

Curr Alzheimer Res. 2014 ; 11(7): 655–663.

Intravenous Immunoglobulin Reduces Tau Pathology and Preserves Neuroplastic Gene Expression in the 3xTg Mouse Model of Alzheimer's Disease

Scott E. Counts[*], **Sylvia E. Perez**, **Bin He**, and **Elliott J. Mufson**

Department of Neurological Sciences, Rush University Medical Center, Chicago, IL 60612 USA

Abstract

Despite recent negative results of the Gammaglobulin Alzheimer's Partnership (GAP) trial, the good tolerability to intravenous immunoglobulin (IVIG) and its potential benefit for patient subpopulations have highlighted the importance of understanding IVIG's mechanism of action. IVIG contains antibodies to amyloid suggesting an amyloid clearance mechanism. However, the suboptimal results of the amyloid immunotherapy trials suggest an additional mechanism. Therefore, we tested whether IVIG alters the expression of tau neurofibrillary tangle (NFT)-like deposits within hippocampal CA1 neurons of the 3xTg mouse model of AD. Three-month-old mice were treated intravenously with IVIG (10%, 400 mg/kg) or placebo (10% BSA/saline) every two weeks for either three or six months. At sacrifice, plasma was isolated for gene expression profiling and brains were processed for immunohistochemistry using the AT-180 antibody, which recognizes hyperphosphorylated tau in NFTs. Stereologic analysis of CA1 neurons following three months of treatment revealed no difference in AT-180+ neuron number but a significant 15–20% decrease in AT-180 intraneuronal optical density with IVIG compared to placebo. By contrast, the number of AT-180+ CA1 neurons was reduced by 25–30% following six months of IVIG treatment compared to placebo. Expression profiling studies showed that IVIG treatment resulted in a significant 40–50% increase in plasma levels of genes regulating neuronal cytoskeletal plasticity function and calcium-mediated signaling compared to placebo. Moreover, several transcripts encoding protein phosphatase subunits were 40–50% higher in IVIG-treated mice. Hence, IVIG reduces hippocampal NFT pathology in the 3xTg mouse through a mechanism that may involve preservation of neuronal plasticity and tau phosphorylation homeostasis.

Keywords

Alzheimer; gene array; hippocampus; immunoglobulin; neurofibrillary tangle; neuroplasticity; therapy

[*]Address correspondence to this author at the Department of Translational Science and Molecular Medicine, Department of Family Medicine, Michigan State University, 333 Bostwick Ave NE, Grand Rapids, MI 49503, USA; Tel: 616-234-0997; Fax: 616-234-0990; scott.counts@hc.msu.edu.

CONFLICT OF INTEREST

The authors confirm that this article content has no conflict of interest.

Author Manuscript Author Manuscript Author Manuscript Author Manuscript

INTRODUCTION

Current treatment options for Alzheimer's disease (AD) offer short-term clinical benefits but fail to alter disease progression. Given the projected three-fold rise in the prevalence of AD over the next few decades (http://www.alz.org/alzheimers_disease_trajectory.asp), the need to identify disease-modifying therapies that prevent selective neuronal vulnerability within memory circuits and halt the onset of symptomatic disease has become critical. While the causes of selective neuronal vulnerability in AD remain unresolved, the disease is characterized neuropathologically by the deposition of extracellular senile plaques (SPs) and accumulation of intraneuronal tau inclusions resulting in neurofibrillary tangles (NFTs), particularly within the hippocampal complex that mediates memory function. Although the prevailing hypothesis is that AD is caused by the deleterious accumulation of amyloid-β (Abeta) peptides [1], the core constituents of SPs, immunotherapeutic strategies targeting Abeta have failed to improve cognition in people with mild AD [2, 3] and these clinical trials resulted in severe adverse effects [4]. More recently, intravenous immunoglobulin (IVIG) therapy has emerged as an alternative immunotherapy which may represent a significant advance over amyloid-based strategies [5, 6]. Specifically, placebo-controlled, double-blind phase II clinical trials with the IVIG preparation Gammagard demonstrated good tolerability and improved cognitive outcomes in patients with mild/moderate AD [6, 7]. However, a recent multicenter double-blinded Phase III study of 390 subjects, called the Gammaglobulin Alzheimer's Partnership (GAP), did not meet primary endpoints of slowing cognitive and functional decline. Then again, the GAP study results continued to support IVIG's positive safety profile and showed potentially beneficial effects for pre-specified moderate AD and apoE4 carrier subgroups (http://www.baxter.com/press_room/press_releases/2013/05_07_13_gap_study.html). Hence, the mechanism of action for IVIG is still of considerable interest in the field. Notably, preclinical studies have demonstrated that IVIG reduces amyloid pathology and associated inflammation in AD transgenic mice [8–10]. However, the failure of Abeta-targeted immunotherapy to improve clinical outcomes raises the possibility that IVIG therapy also acts via an amyloid-independent mechanism that prevents cytopathology [5]. Therefore, we tested the extent to which IVIG alters the expression of select NFT tau epitopes within hippocampal CA1 pyramidal neurons of the 3xTg mouse model of AD, which displays both intracellular amyloid and tau cytoskeletal inclusions [11]. In addition to evaluating the effects of IVIG therapy on NFT cytopathology, we also compared gene expression profiles of plasma isolated from placebo and IVIG-treated 3xTg mice to identify putative mechanistic markers for the pathogenic events underlying disease progression and the therapeutic modification of these events by IVIG.

METHODS

Animals

3xTg mice, a well-established mouse model for AD bearing human mutant APPswe, PS1M146V, and TauP301L transgenes [11], were bred and treated using protocols which were approved by the Rush University Medical Center Institutional Animal Care and Use Committee.

Author Manuscript Author Manuscript Author Manuscript Author Manuscript

Treatment Design

We have previously reported that hippocampal NFT and amyloid pathology begins to accumulate from 3 to 9 months of age in these mice with a gender-specific acceleration of pathology in the female mice [12]. As such, three month-old female 3xTg mice were randomized into experimental and placebo groups. Experimental groups (n = 15/group) received 400 mg/kg bodyweight of Gammagard, 10% (Baxter Healthcare) intravenously via the retro-orbital sinus every two weeks under anesthesia. This dosage was consistent with dosage levels tested in Phase III trials. The placebo group received injections of 10% heat-inactivated bovine serum albumin (Sigma) in saline. Prior to injection, an equivalent volume of blood was drawn from the sinus and serum was prepared by centrifugation at 12,000 × *g* for five minutes at room temperature. Serum samples were shipped to Baxter (Round Lake, IL) for anti-human Ig titer analysis. From the first cohort of experimental and placebo groups, 12 from each group completed the regimen and were sacrificed at six months of age (i.e., after six injections); from the second cohort, 11–13 from each group completed the regimen and were sacrificed at nine months of age (i.e., after 12 injections). A baseline cohort (three months old, no treatment, n = 8) was also evaluated.

Strategy for Quantifying IVIG Effects of Tangle Pathology

Female mice were sacrificed during proestrus to preclude the effects of hormonal status [12–14]. Mice were transcardially perfused with saline and brains from each group were hemisected. One hemisphere was immersion-fixed in 4% paraformaldehyde/0.1% glutaraldehyde for 24 hours and stored in cryoprotectant. From the other hemisphere, hippocampus, frontoparietal cortex, and cerebellum were rapidly dissected and snap-frozen [12–14].

A full series of 40 μm-thick fixed tissue sections containing the full extent of the hippocampus was cut on a freezing-sliding microtome. For immunostochemistry, sections were blocked in Tris-buffered saline (TBS, pH 7.4) containing 0.25% Triton X-100 and 3% goat serum, followed by overnight incubation at room temperature with the AT-180 monoclonal mouse antibody (1:1000, Thermo Scientific) in TBS/0.25% TX-100/1% goat serum. The AT-180 antibody labels the tau T231 phosphoepitope associated with NFTs in the AD brain [15]. Tissue from each time point was immunostained at the same time to mitigate batch effects. An observer blinded to treatment performed unbiased cell counts of AT-180+ CA1 pyramidal neurons in six serial sections using optical disector stereology (Stereo Investigator, Williston, VT), as previously described [16–20]. Optical density measurements of AT-180+ immunoreactivity within individual CA1 neurons were performed across six serial sections/mouse using NIH Image software. Sections were also immunostained with the Alz50 tau conformational antibody (a gift from Peter Davies, Einstein College of Medicine, NY). Adjacent sections were immunostained with 6E10 (1:500, Covance) or GFAP (1:1000, Chemicon/Millipore) to evaluate the presence of Abeta and reactive astrocyte accumulation, respectively.

Quantitative Immunoblotting

Frozen hippocampi were sonicated in extraction buffer (10 mM Tris/1 mM EGTA/800 mM NaCl/10% sucrose, pH 7.4) with protease/phosphatase inhibitors and centrifuged at 18,000 ×

Author Manuscript Author Manuscript Author Manuscript Author Manuscript

g for 45 minutes at 4°C. TBS-extracted, S1 fraction proteins (25 μg/sample) were separated by SDS-PAGE, transferred to Immobilon P membranes (Millipore, MA), blocked in Tris-buffered saline (TBS, pH.7.4)/0.1% Tween-20/5% milk, and incubated overnight at 4°C with the AT-180 mouse antibody (1:1000). Membranes were also incubated with mouse anti β-actin (Chemicon, 1:20,000) as the loading control. Blots were incubated for 1 hour with horseradish peroxidase-conjugated goat anti-mouse IgG secondary antibody (1:8,000; Pierce, IL) and reactivity was quantified using Kodak 1D image analysis software (Perkin-Elmer, MA). Blots were stripped for 15 min at room temperature (Restore Buffer, Pierce) and reprobed with tau5 (1:100,000, a gift from Dr. Skip Binder, Northwestern University) to measure total tau levels.

Plasma Collection

Cardiac puncture of the right ventricle was performed to draw ~300 μl blood prior to perfusion of each animal. Animals were fasted overnight prior to sacrifice to control for metabolic fluctuations. Blood was drawn into EDTA-treated tubes and immediately spun at 1500 rpm for 10 min at 4 °C to separate the plasma, buffy coat, and erythrocyte fractions. Plasma was snap-frozen and stored at −80 °C.

Plasma mRNA Amplification and Custom Microarray

Analysis—mRNA from collected plasma fractions was extracted in Trizol (Life Tech) and amplified using terminal continuation (TC) RNA amplification methodology, as previously reported [21–24]. A detailed description of this method can be found at http://cdr.rfmh.org/Labgoups/ginsberg_protocol.html. The last step of the process uses neuronal cDNA as a template to synthesize radiolabeled hybridization probes by *in vitro* transcription. This is a linear amplification process that preserves the original quantitative relationships among the transcripts [25]. Probes are then hybridized to custom-designed microarrays with 576 cDNAs encoding functional gene classes mediating critical cellular pathways [26–28]. Each array was analyzed on a Storm phosphor imager with ImageQuant software (GE, Piscataway, NJ). RNA bound to each cDNA was expressed as a ratio of the total hybridization signal intensity of the array (i.e., global normalization)[26, 27, 29–31], thereby minimizing variations due to differences in the specific activity of the probe and the absolute quantity of probe present [25, 28, 30, 32]. Data analysis generated expression profiles of the relative changes in mRNA levels for quantitative comparison among baseline, IVIG- and placebo-treated animals.

Statistical Analysis

NFT counts, optical density and immunoblot measurements were compared between the IVIG and placebo groups at each treatment time point using unpaired Student's *t* tests, whereas comparisons of NFT variables between the two treatment groups over time were analyzed by two-way ANOVA. Spearman rank correlations were used to test for associations between length of treatment and NFT pathologic variables. The relationship between NFT variables and human Ig titer responses in the mice were assessed by Spearman rank correlations. The level of significance was set at = 0.05 (two-tailed).

Author Manuscript Author Manuscript Author Manuscript Author Manuscript

For plasma profiling analysis, relative changes in mean hybridization signal intensity for individual mRNAs among the baseline, placebo, and IVIG groups was compared using one-way ANOVA with Bonferroni's *post hoc* test for multiple comparisons. Expression levels were analyzed using Gene Linker bioinformatics software (IOS, Kingston, ON). P-values were adjusted using a false discovery rate controlling procedure [33] to reduce type I error due to the large number of genes analyzed simultaneously. The level of significance was set at $\alpha = 0.01$ (two-tailed). Relationships between transcript levels and NFT variables were assessed by Spearman rank correlations.

RESULTS

Three Months of IVIG Treatment Reduces AT-180 Tau Pathology within CA1 Pyramidal Neurons in 3xTg Mice

Three month old mice in the three month treatment arm received placebo or 400 mg/kg IVIG every two weeks and were sacrificed at six months of age. AT-180 immunostaining of hippocampal sections revealed relatively lighter labeling of CA1 pyramidal cells and fibers in the IVIG group (Fig. 1B, D) compared to placebo (Fig. 1 A,C). Unbiased stereologic counts of CA1 pyramidal neurons immunostained for AT-180 did not show any differences between the two groups (Fig. 1E). However, optical densitometric analysis revealed a significant 15–20% reduction in CA1 intracellular AT-180 intensity (Fig. 1F). We found similar reductions in optical density at this time point using the AD-related Alz50 conformational tau antibody (not shown).

Six Months of IVIG Treatment Reduces the Number of AT-180-Immunoreactive CA1 Pyramidal Neurons in 3xTg Mice

Three month old mice in the six month treatment arm received placebo or 400 mg/kg IVIG every two weeks and were sacrificed at nine months of age. At this time point, the number of AT-180-immunoreactive CA1 neurons was reduced by 25–30% in the IVIG group compared to placebo, whereas CA1 intracellular AT-180 staining intensity was equivalent between the two groups (Fig. 2). There were no statistically significant interactions between treatment type and treatment duration for the stereologic or optical density measurements. Quantitative immunoblotting of frozen hippocampal tissue from the same mice validated the observed reduction in AT-180 by stereology and verified that decreased levels of AT-180 epitopes were not secondary to an IVIG-mediated reduction in total tau (Fig. 3).

IVIG Treatment Effects on Amyloid and Inflammatory Pathology

Sections adjacent to those used for AT-180 analysis were immunostained for A beta-related pathology using the 6E10 antibody. No plaque-like deposits were evident in the three or six month treatment groups; however, we observed a substantial increase in intraneuronal and neuropil 6E10 staining in the CA1 field of placebo-treated mice that was substantially diminished with IVIG treatment after three (Fig. 4A,B) or six (Fig. 4C,D) months. We noted a similar effect of IVIG treatment on CA1 expression of glial fibrillary acidic protein (GFAP), a marker for inflammatory astrogliosis (Fig. 4E,F).

Author Manuscript Author Manuscript Author Manuscript Author Manuscript

Gene Classes Regulating Cytoskeletal Plasticity and Calcium Signaling Pathways are Preserved in IVIG-Treated 3xTg-AD Mice

Plasma gene expression profiling was performed using custom microarrays following TC RNA amplification. Relative hybridization signal intensities for each cDNA on the arrays were compared among the placebo and IVIG-treated 3xTg mice and transgenic littermates sacrificed at three months of age as a baseline control group. Quantitative analysis at three months revealed 40–50% reductions in the expression levels of several gene clusters regulating cytoskeletal plasticity in the placebo groups relative to the IVIG-treated group. These transcripts included microtubule-associated protein 1b (MAP1b), neurofilament heavy chain subunit (NEFH), A kinase anchor protein (AKAP), nestin (NES), Homer1 (HOMER1), and activity-regulated cytoskeletal-associated protein (ARC) (Fig. 5A). Notably, levels of these mRNAs were similar between the IVIG and baseline groups, suggesting a preservation of cytoskeletal integrity with IVIG treatment relative to placebo. With the exception of MAP1b and HOMER1, IVIG treatment continued to stabilize levels of the cytoskeletal markers in the six month treatment group (Fig. 5B).

The microarray data was also queried for intracellular signaling pathways which might be preserved with IVIG treatment in the 3xTg mice. Whereas certain canonical prosurvival second messenger molecules such as extracellular signal regulated kinase 1 (ERK1), v-akt viral oncogene homolog 1 (AKT1), and cAMP-response element binding protein (CREB) were unchanged, three months of IVIG did prevent a significant 35–45% reduction in plasma levels of select mRNAs regulating calcium-dependent intracellular signaling, synaptic plasticity, and cell survival, including calcium/calmodulin-mediated protein kinase 2 alpha (CAMK2A), protein kinase C alpha (PRKCA), protein kinase C iota (PRKCI), and the inositol triphosphate kinases A and B (ITPKA and ITPKB) (Fig. 6A). By contrast, IVIG prevented a 35% increase in plasma levels of N-type voltage-gated calcium channel transcripts (CACNA1B) (Fig. 6A). Analysis of the same transcripts after six months of IVIG treatment revealed a similar pattern for the calcium signaling molecules (Fig. 6B). In addition, IVIG also prevented a significant 30% loss of CREB mRNA levels at this time point (Fig. 6B), suggesting the involvement of multiple intracellular second messenger cascades in IVIG reduction of AT-180-positive CA1 pyramidal neurons at the six month treatment time point (Fig. 2).

Protein Phosphatase Gene Expression is Elevated in Plasma of Six Month IVIG-Treated 3xTg-AD Mice

Since AT-180 recognizes a tau phosphoepitope, datasets were also queried for evidence of protein phosphatase regulation which might mitigate the formation of this epitope during IVIG treatment. Notably, at the six month treatment time point, several classes of phosphatase enzyme subunits present on the arrays were significantly increased 40–50% with IVIG compared to placebo or baseline (Fig. 7). These included protein phosphatase 1, catalytic subunit, alpha isozyme (PPP1CA); protein phosphatase 1, catalytic subunit, gamma isozyme (PPP1CG); protein phosphatase 2, regulatory subunit A, alpha (PPP2R1A); protein phosphatase 2, catalytic subunit, alpha isozyme (PPP2CA); and protein phosphatase 3, catalytic subunit, beta isozyme (PPP3CB).

Author Manuscript Author Manuscript Author Manuscript Author Manuscript

Correlations with Anti-Human Ig Titer Responses

Seventy-seven percent of mice treated with IVIG developed detectable IgG antibody titers in serum which ranged from 1–64. Correlation analysis did not reveal significant associations between serum anti-human IgG titer and the stereologic or gene expression variables in these mice after three or six months of treatment (data not shown).

DISCUSSION

Although the GAP trial did not meet its primary endpoints, the good safety profile for IVIG and its potential benefit for pre-specified patient subpopulations have focused further attention on understanding IVIG's mechanism of action. The presence of circulating anti-Aβ antibodies in IVIG [34] suggests that it acts similar to amyloid immunotherapy[8]. In this regard, the GAP study also revealed a dose-dependent increase in cerebrospinal fluid levels of Abeta antibodies and a reduction in plasma levels of Abeta in IVIG- treated patients relative to placebo (http://www.baxter.com/press_room/press_releases/2013/07_16_13_aaic_gap_data.html). On the other hand, the role of IVIG in immune modulation for the treatment of autoimmune disorders suggests an anti-inflammatory role [5]. More recently, it has been shown that intracranial injections of IVIG lowers brain Abeta in APPSwe/PS1ΔE9 mice by comparable degrees as that seen with injections of 6E10 antibody, albeit by a slower time course [10]. Further analysis revealed that IVIG administration promoted a switch from an M2a to M2b inflammatory phenotype prior to Abeta reduction, suggesting an immune modulatory mechanism [10]. By contrast, another study using APPSwe/PS1ΔE9 mice found that intraperitoneal injections of IVIG did not reduce amyloid burden, but rather increased soluble levels of Abeta concomitant with a significant elevation of Iba-1 positive microglia and suppression of TNF-α, providing further evidence that the immunogenic activity of IVIG may impact amyloid metabolism. However, despite this focus on amyloid-dependent mechanisms for therapeutic efficacy, the deleterious results of recent phase III trials targeting Abeta suggest that IVIG could also act by additional mechanisms. Here, we demonstrate that IVIG also impacts the accumulation of hyperphosphorylated tau into NFT-like deposits within the hippocampus of 3xTg mice.

Our stereologic analysis of hippocampal CA1 pyramidal neurons following three or six months of intravenous IVIG or placebo treatment revealed that initial reductions in AT-180 optical density within individual neurons (three months treatment) ultimately resulted in a reduction in the number of CA1 neurons bearing AT-180 tau pathology (six months treatment). Hence, IVIG appears to exert a beneficial effect on the accumulation of NFT-like pathology in this mutant APP/PS1/tau AD mouse model in addition to its beneficial effects on Abeta pathology in APP/PS1 mice, which do not express mutant tau and are not engineered to examine NFTs. In this regard, the present study adds IVIG to a very small list of other FDA-approved drugs, including lithium [35], pioglitazone [36], and nicotinamide [37], which are capable of reducing NFT pathology in preclinical mouse models.

The mechanism of action whereby IVIG might exert its effects on tau pathology is unclear. To address this problem, we performed plasma gene expression profiling on the same animals used in our stereologic studies of CA1 NFTs. Data mining of our custom microarray data revealed that transcript levels of several classes of genes regulating cytoskeletal

Author Manuscript Author Manuscript Author Manuscript Author Manuscript

plasticity function in axonal maintenance, including MAP1b, neurofilament H, and nestin were preserved relative to baseline with either three or six months IVIG treatment. While these measurements were made from plasma, they indicate that 3xTg mice undergo significant age-dependent destabilization of cytoskeletal components, possibly driven by mutant tau overexpression, and that IVIG acts to preserve cytoskeletal integrity such that these mutant tau pathological processes are slowed down over time, resulting in fewer NFT-bearing CA1 neurons.

We also discovered two other major IVIG-mediated alterations in the genetic signature of 3xTg mouse plasma following treatments. First, several mRNAs encoding calcium-mediated signaling involved in synaptic plasticity and survival, including CAMK2A, which is required for long term potentiation and memory in rodents [38], as well as protein kinase C isoforms [39], were preserved with IVIG compared to baseline, while these same molecules were down-regulated in placebo-treated mice over time. Calcium signaling is crucial for many aspects of plasticity at glutamatergic synapses [40], indicating that the potential restorative properties of IVIG for maintaining calcium homeostasis is critical for preserved function within CA1 glutamatergic circuits. This neuroplastic maintenance function of IVIG in the 3xTg hippocampus is reminiscent of recent observations that IVIG increases doublecortin positive adult-born neurons in the dentate gyrus of APP/PS1 mice [9].

Protein phosphatase subunits comprised the second major group of transcripts regulated by IVIG. Specifically, both regulatory and catalytic subunits of protein phosphatases PPP1, PPP2, and PPP3 were all increased by IVIG in the six month treatment group compared to baseline and placebo. Given the direct role for these molecules, particularly PPP1 and PPP2, in dephosphorylating tau [41, 42], their upregulation by IVIG provides the most direct route whereby IVIG might slow the intracellular formation of AT-180 tau pathology in CA1 pyramidal neurons over time, resulting in fewer CA1 neurons bearing this NFT epitope.

CONCLUSION

In summary, we show that IVIG abrogates the age-dependent hippocampal tau pathological burden observed in the 3xTg mouse model of AD. Moreover, our gene expression profiling experiments revealed that IVIG may slow tangle propagation by stabilizing or increasing cytoskeletal and calcium signaling plasticity and phosphorylation-based cellular homeostatic mechanisms in the face of mounting AD pathology in these mice. Future studies will determine the extent to which these plasma biomarker changes are reflected in the hippocampus of these mice. The extent to which IVIG's effects on Abeta and inflammation (Fig. 4) impact the observed changes in tau pathology or gene expression will require further investigation. For instance, Abeta antibody depletion of IVIG may show whether or not the present observations are secondary to or independent of Abeta reduction. Nonetheless, the data presented suggest that IVIG is a useful tool for understanding the mechanisms of NFT formation and prevention that will aid in the further design of IVIG clinical trials for the treatment of AD.

Author Manuscript Author Manuscript Author Manuscript Author Manuscript

ACKNOWLEDGEMENTS

The authors would like to thank Dr. Yinzhen He (Rush University Medical Center) for expert technical assistance, Dr. Deborah Kasprowicz (Baxter Biosciences) for human Ig analysis, and Dr. Michelle Gilmor (Baxter Biosciences) for helpful discussions during the study. This study was funded by an Investigator Initiated Award from Baxter Biosciences (SEC).

REFERENCES

[1]. Selkoe DJ. Preventing Alzheimer's disease. Science 337: 1488–92 (2012). [PubMed: 22997326]

[2]. Holmes C, Boche D, Wilkinson D, Yadegarfar G, Hopkins V, Bayer A, et al. Long-term effects of Abeta42 immunisation in Alzheimer's disease: follow-up of a randomised, placebo-controlled phase I trial. Lancet 372: 216–23 (2008). [PubMed: 18640458]

[3]. Salloway S, Sperling R, Gilman S, Fox NC, Blennow K, Raskind M, et al. A phase 2 multiple ascending dose trial of bapineuzumab in mild to moderate Alzheimer disease. Neurology 73: 2061–70 (2009). [PubMed: 19923550]

[4]. Gilman S, Koller M, Black RS, Jenkins L, Griffith SG, Fox NC, et al. Clinical effects of Abeta immunization (AN1792) in patients with AD in an interrupted trial. Neurology 64: 1553–62 (2005). [PubMed: 15883316]

[5]. Dodel R, Neff F, Noelker C, Pul R, Du Y, Bacher M, et al. Intravenous immunoglobulins as a treatment for Alzheimer's disease: rationale and current evidence. Drugs 70: 513–28 [PubMed: 20329802]

[6]. Relkin NR, Szabo P, Adamiak B, Burgut T, Monthe C, Lent RW, et al. 18-Month study of intravenous immunoglobulin for treatment of mild Alzheimer disease. Neurobiol Aging 30: 1728–36 (2009). [PubMed: 18294736]

[7]. Relkin NR, Tsakanikis DI, Adamiak B. A double-blind, placebo-controlled phase II clinical trial of intravenous immunoglobulin (IVIG) for treatment of Alzheimer's disease. Neurology 70: A393 (2008).

[8]. Magga J, Puli L, Pihlaja R, Kanninen K, Neulamaa S, Malm T, et al. Human intravenous immunoglobulin provides protection against Abeta toxicity by multiple mechanisms in a mouse model of Alzheimer's disease. J Neuroinflammation 7: 90 (2010). [PubMed: 21138577]

[9]. Puli L, Pomeshchik Y, Olas K, Malm T, Koistinaho J, Tanila H. Effects of human intravenous immunoglobulin on amyloid pathology and neuroinflammation in a mouse model of Alzheimer's disease. J Neuroinflammation 9: 105 (2012). [PubMed: 22642812]

[10]. Sudduth TL, Greenstein A, Wilcock DM. Intracranial injection of Gammagard, a human IVIg, modulates the inflammatory response of the brain and lowers Abeta in APP/PS1 mice along a different time course than anti-Abeta antibodies. J Neurosci 33: 9684–92 (2013). [PubMed: 23739965]

[11]. Oddo S, Caccamo A, Shepherd JD, Murphy MP, Golde TE, Kayed R, et al. Triple-transgenic model of Alzheimer's disease with plaques and tangles: intracellular Abeta and synaptic dysfunction. Neuron 39: 409–21 (2003). [PubMed: 12895417]

[12]. Oh KJ, Perez SE, Lagalwar S, Vana L, Binder L, Mufson EJ. Staging of Alzheimer's pathology in triple transgenic mice: a light and electron microscopic analysis. Int J Alzheimers Dis in press: (2010).

[13]. Perez SE, Berg BM, Moore KA, He B, Counts SE, Fritz JJ, et al. DHA diet reduces AD pathology in young APPswe/PS1 Delta E9 transgenic mice: possible gender effects. J Neurosci Res 88: 1026–40 (2010). [PubMed: 19859965]

[14]. Perez SE, He B, Muhammad N, Oh KJ, Fahnestock M, Ikonomovic MD, et al. Cholinotrophic basal forebrain system alterations in 3xTg-AD transgenic mice. Neurobiol Dis

[15]. Mercken M, Vandermeeren M, Lubke U, Six J, Boons J, Van de Voorde A, et al. Monoclonal antibodies with selective specificity for Alzheimer Tau are directed against phosphatase-sensitive epitopes. Acta Neuropathol 84: 265–72 (1992). [PubMed: 1384266]

[16]. Chu Y, Le W, Kompoliti K, Jankovic J, Mufson EJ, Kordower JH. Nurr1 in Parkinson's disease and related disorders. J Comp Neurol 494: 495–514 (2006). [PubMed: 16320253]

Author Manuscript Author Manuscript Author Manuscript Author Manuscript

[17]. Gilmor ML, Erickson JD, Varoqui H, Hersh LB, Bennett DA, Cochran EJ, et al. Preservation of nucleus basalis neurons containing choline acetyltransferase and the vesicular acetylcholine transporter in the elderly with mild cognitive impairment and early Alzheimer's disease. J Comp Neurol 411: 693–704. (1999). [PubMed: 10421878]

[18]. Kordower JH, Chu Y, Stebbins GT, DeKosky ST, Cochran EJ, Bennett D, et al. Loss and atrophy of layer II entorhinal cortex neurons in elderly people with mild cognitive impairment. Ann Neurol 49: 202–13. (2001). [PubMed: 11220740]

[19]. Mufson EJ, Ma SY, Cochran EJ, Bennett DA, Beckett LA, Jaffar S, et al. Loss of nucleus basalis neurons containing trkA immunoreactivity in individuals with mild cognitive impairment and early Alzheimer's disease. J Comp Neurol 427: 19–30. (2000). [PubMed: 11042589]

[20]. Mufson EJ, Ma SY, Dills J, Cochran EJ, Leurgans S, Wuu J, et al. Loss of basal forebrain P75(NTR) immunoreactivity in subjects with mild cognitive impairment and Alzheimer's disease. J Comp Neurol 443: 136–53. (2002). [PubMed: 11793352]

[21]. Che S, Ginsberg SD. Amplification of RNA transcripts using terminal continuation. Lab Invest 84: 131–7 (2004). [PubMed: 14647400]

[22]. Counts SE, He B, Che S, Ginsberg SD, Mufson EJ. Galanin fiber hyperinnervation preserves neuroprotective gene expression in cholinergic basal forebrain neurons in Alzheimer's disease. J Alzheimers Dis 18: 885–96 (2009). [PubMed: 19749437]

[23]. Counts SE, He B, Che S, Ikonomovic MD, DeKosky ST, Ginsberg SD, et al. Alpha7 nicotinic receptor up-regulation in cholinergic basal forebrain neurons in Alzheimer disease. Arch Neurol 64: 1771–6 (2007). [PubMed: 18071042]

[24]. Ginsberg SD, Alldred MJ, Counts SE, Cataldo AM, Neve RL, Jiang Y, et al. Microarray analysis of hippocampal CA1 neurons implicates early endosomal dysfunction during Alzheimer's disease progression. Biol Psychiatry 68: 885–93 (2010). [PubMed: 20655510]

[25]. Ginsberg SD, Hemby SE, Lee VM, Eberwine JH, Trojanowski JQ. Expression profile of transcripts in Alzheimer's disease tanglebearing CA1 neurons. Ann Neurol 48: 77–87. (2000). [PubMed: 10894219]

[26]. Ginsberg SD, Che S. Combined histochemical staining, RNA amplification, regional, and single cell cDNA analysis within the hippocampus. Lab Invest 84: 952–62 (2004). [PubMed: 15107803]

[27]. Ginsberg SD, Elarova I, Ruben M, Tan F, Counts SE, Eberwine JH, et al. Single-cell gene expression analysis: implications for neurodegenerative and neuropsychiatric disorders. Neurochem Res 29: 1053–64 (2004). [PubMed: 15176463]

[28]. Ginsberg SD. RNA amplification strategies for small sample populations. Methods 37: 229–37 (2005). [PubMed: 16308152]

[29]. Eberwine J, Kacharmina JE, Andrews C, Miyashiro K, McIntosh T, Becker K, et al. mRna expression analysis of tissue sections and single cells. J Neurosci 21: 8310–4. (2001). [PubMed: 11606616]

[30]. Hemby SE, Trojanowski JQ, Ginsberg SD. Neuron-specific age-related decreases in dopamine receptor subtype mRNAs. J Comp Neurol 456: 176–83. (2003). [PubMed: 12509874]

[31]. Hemby SE, Ginsberg SD, Brunk B, Arnold SE, Trojanowski JQ, Eberwine JH. Gene expression profile for schizophrenia: discrete neuron transcription patterns in the entorhinal cortex. Arch Gen Psychiatry 59: 631–40 (2002). [PubMed: 12090816]

[32]. Ginsberg SD, Crino PB, Hemby SE, Weingarten JA, Lee VM, Eberwine JH, et al. Predominance of neuronal mRNAs in individual Alzheimer's disease senile plaques. Ann Neurol 45: 174–81. (1999). [PubMed: 9989619]

[33]. Reiner A, Yekutieli D, Benjamini Y. Identifying differentially expressed genes using false discovery rate controlling procedures. Bioinformatics 19: 368–75. (2003). [PubMed: 12584122]

[34]. Dodel R, Hampel H, Depboylu C, Lin S, Gao F, Schock S, et al. Human antibodies against amyloid beta peptide: a potential treatment for Alzheimer's disease. Ann Neurol 52: 253–6 (2002). [PubMed: 12210803]

[35]. Caccamo A, Oddo S, Tran LX, LaFerla FM. Lithium reduces tau phosphorylation but not A beta or working memory deficits in a transgenic model with both plaques and tangles. Am J Pathol 170: 1669–75 (2007). [PubMed: 17456772]

Author Manuscript Author Manuscript Author Manuscript Author Manuscript

[36]. Searcy JL, Phelps JT, Pancani T, Kadish I, Popovic J, Anderson KL, et al. Long-term pioglitazone treatment improves learning and attenuates pathological markers in a mouse model of Alzheimer's disease. J Alzheimers Dis 30: 943–61 (2012). [PubMed: 22495349]

[37]. Green KN, Steffan JS, Martinez-Coria H, Sun X, Schreiber SS, Thompson LM, et al. Nicotinamide restores cognition in Alzheimer's disease transgenic mice via a mechanism involving sirtuin inhibition and selective reduction of Thr231-phosphotau. J Neurosci 28: 11500–10 (2008). [PubMed: 18987186]

[38]. Silva AJ, Stevens CF, Tonegawa S, Wang Y. Deficient hippocampal long-term potentiation in alpha-calcium-calmodulin kinase II mutant mice. Science 257: 201–6 (1992). [PubMed: 1378648]

[39]. Battaini F, Lucchi L, Bergamaschi S, Ladisa V, Trabucchi M, Govoni S. Intracellular signalling in the aging brain. The role of protein kinase C and its calcium-dependent isoforms. Ann N Y Acad Sci 719: 271–84 (1994). [PubMed: 8010599]

[40]. LaFerla FM. Calcium dyshomeostasis and intracellular signalling in Alzheimer's disease. Nat Rev Neurosci 3: 862–72 (2002). [PubMed: 12415294]

[41]. Iqbal K, Alonso Adel C, Chen S, Chohan MO, El-Akkad E, Gong CX, et al. Tau pathology in Alzheimer disease and other tauopathies. Biochim Biophys Acta 1739: 198–210 (2005). [PubMed: 15615638]

[42]. Liu F, Grundke-Iqbal I, Iqbal K, Gong CX. Contributions of protein phosphatases PP1, PP2A, PP2B and PP5 to the regulation of tau phosphorylation. Eur J Neurosci 22: 1942–50 (2005). [PubMed: 16262633]

Author Manuscript Author Manuscript Author Manuscript Author Manuscript

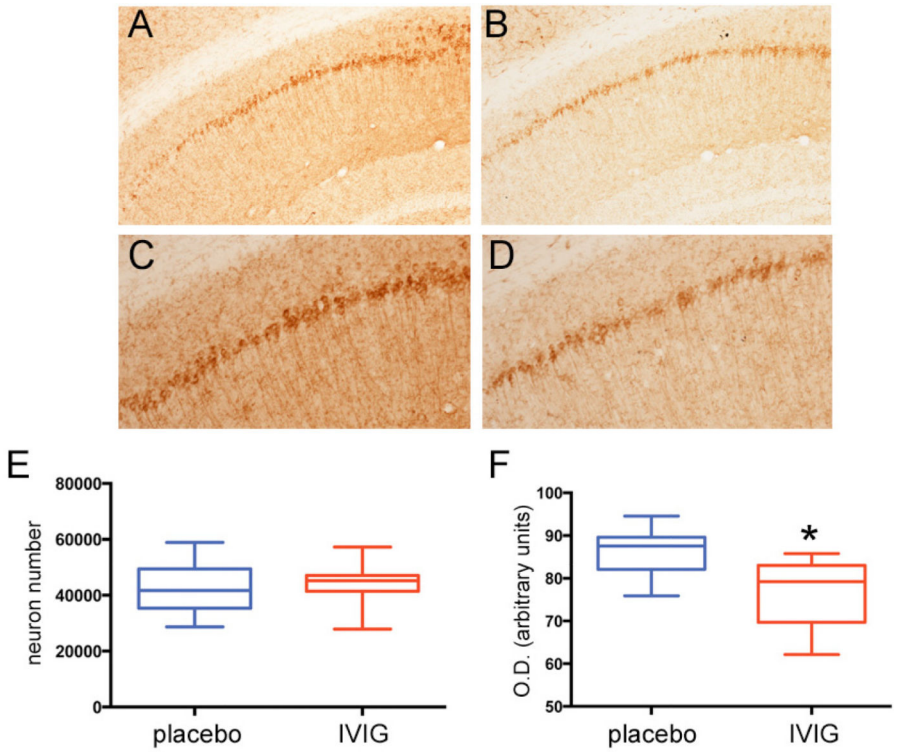

Fig. (1). Three months of IVIG reduces NFT expression levels within CA1 neurons. A-D) Photomicrographs show AT-180 immunolabeling of CA1 pyramidal neurons and fibers in 3xTg mice treated with placebo (**A,C**) or IVIG (**B,D**) for three months. Panels (**C**) and (**D**) are higher magnification photomicrographs of (**A**) and (**B**), respectively. Note the lighter staining in the IVIG-treated mice compared to placebo-treated mice. **E**) Unbiased stereologic cell counts revealed no difference in the number of AT-180+ CA1 neurons between the two groups. **F**) Optical densitometric measurements revealed a significant 15–20% decrease in AT-180 labeling intensity within individual CA1 neurons in IVIG compared to placebo. $n = 12$/group; *, $p < 0.01$ via Student's unpaired t test (two-tailed).

Author Manuscript Author Manuscript Author Manuscript Author Manuscript

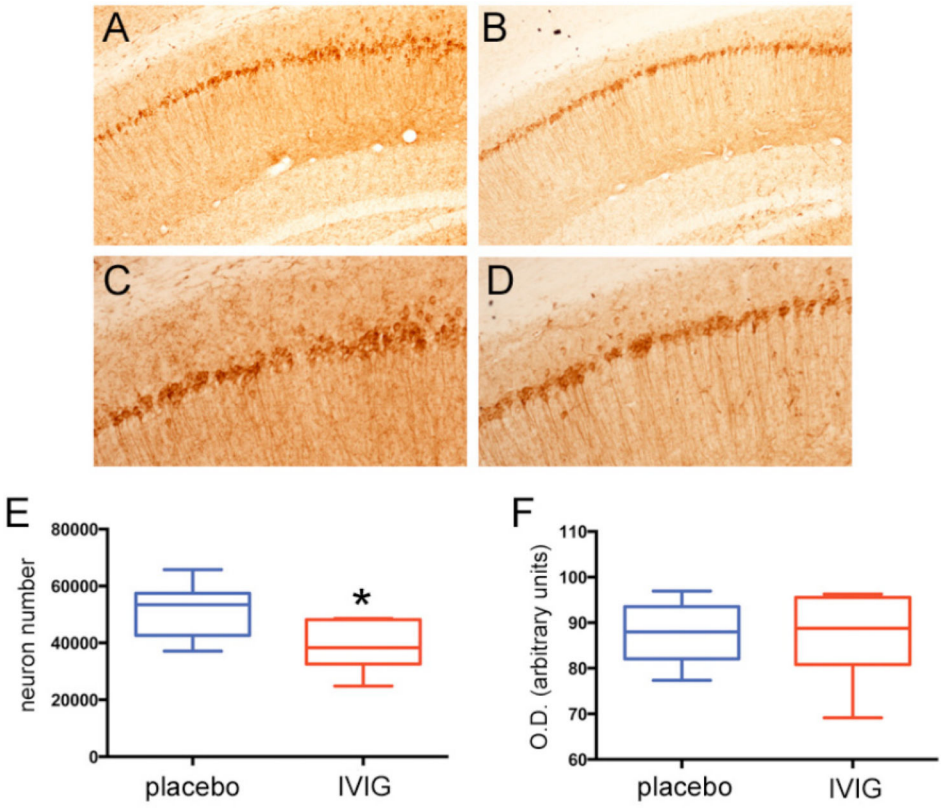

Fig. (2). Six months IVIG reduces the number of NFT-bearing CA1 neurons.

A-D) Photomicrographs show AT-180 immunolabeling of CA1 pyramidal neurons and fibers in 3xTg mice treated with placebo (**A,C**) or IVIG (**B,D**) for six months. Panels (**C**) and (**D**) are higher magnification photomicrographs of (A) and (B), respectively. **E**) Unbiased stereologic cell counts revealed a significant 25–30% reduction in the number of AT-180+ neurons in IVIG compared to placebo-treated mice. **F**) Optical densitometric measurements revealed no differences in AT-180 labeling intensity between the two groups. n = 11–13/group; *, $p < 0.01$ via Student's unpaired t test (two-tailed).

Author Manuscript Author Manuscript Author Manuscript Author Manuscript

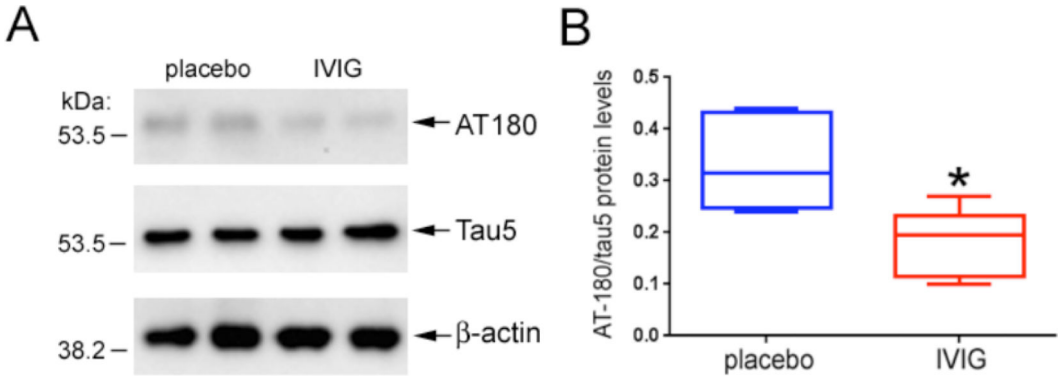

Fig. (3). IVIG does not affect the expression levels of total tau.

A) The immunoblot shows that TBS-extractable total tau levels appear to be equivalent in hippocampal lysates from mice treated with placebo and IVIG for six months. Note that levels of the β-actin loading control are also equivalent in the same samples. On the other hand, tau proteins bearing the AT-180 epitope appear reduced in the IVIG samples compared to placebo. **B**) Quantitative analysis revealed that total tau levels were unchanged between the two treatment groups (not shown), and that hippocampal levels of AT-180 were reduced by ~50% in IVIG relative to placebo. $n = 6$/group; *, $p < 0.01$ via Student's unpaired t test (two-tailed).

Author Manuscript Author Manuscript Author Manuscript Author Manuscript

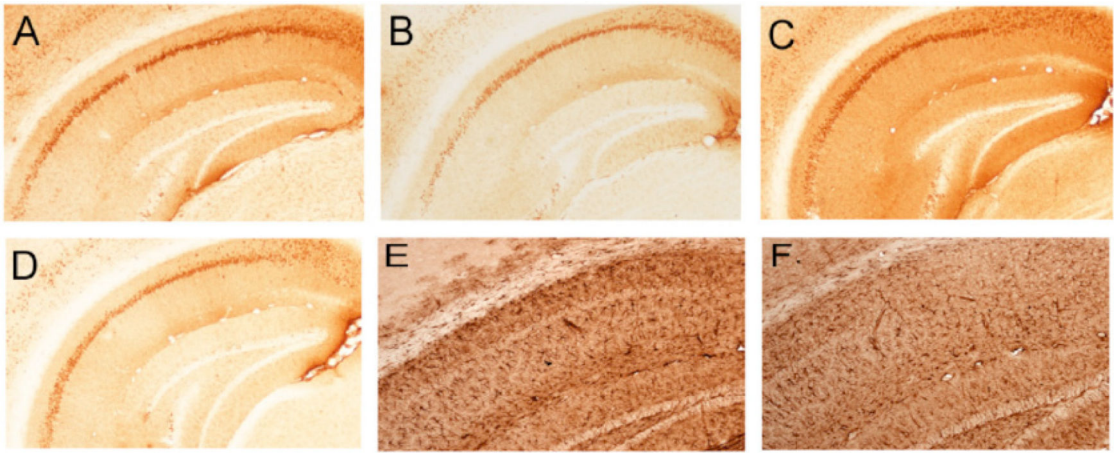

Fig. (4). IVIG effects on hippocampal intracellular amyloid and astroglial pathology.

A-D) Photomicrographs show immunolabeling of CA1 neurons and fibers with the 6E10 antibody raised against the N-terminus of Abeta. Intraneuronal amyloid accumulation was observed following three months of placebo (**A**) or IVIG (**B**) treatment. Note the relatively lighter cellular and neuropilstaining in the IVIG treated group. Intraneuronal Abeta continued to accumulate following six months of placebo (**C**) treatment but remained diminished with IVIG (**D**) treatment. **E,F**) Photomicrographs show GFAP immunolabeling of astroglia in the hippocampal CA1 region in the placebo (**E**) and IVIG (**F**) groups after three months treatment. Note the relatively lighter staining in IVIG compared to placebo. This differential staining pattern continued in the six month treatment groups (not shown).

Author Manuscript Author Manuscript Author Manuscript Author Manuscript

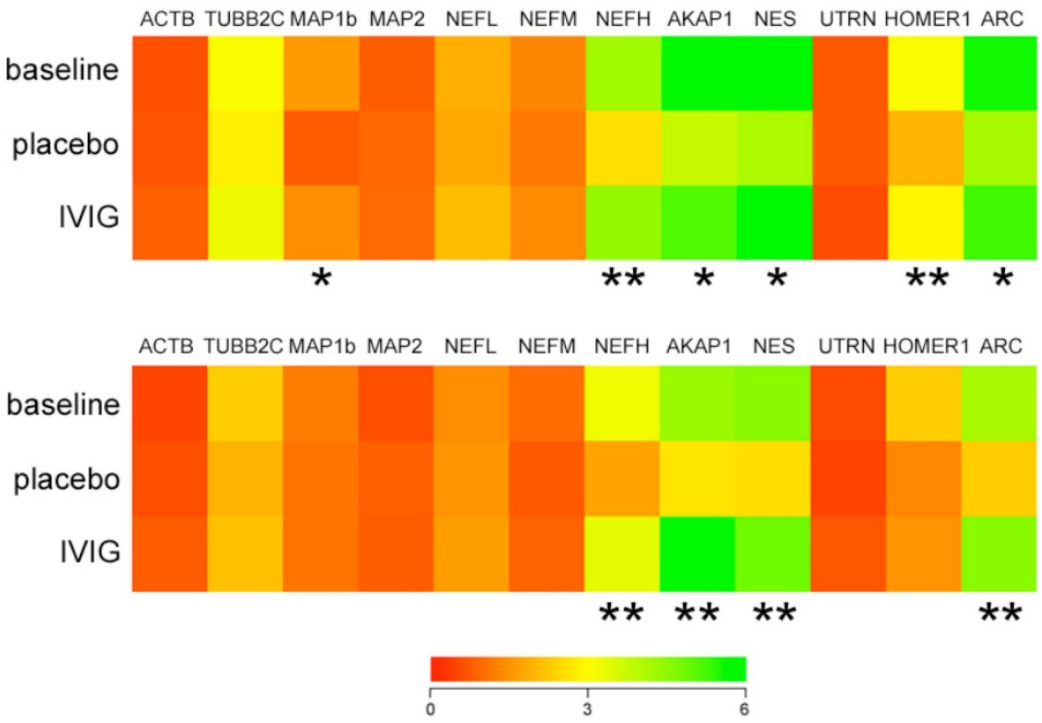

Fig. (5). IVIG regulates plasma levels of cytoskeletal plasticity mRNAs.

A) Three months of IVIG preserved plasma levels of select mRNAs regulating cytoskeletal function. Heat map (red to green = increasing mRNA levels) shows that, compared to placebo, IVIG treatment resulted in 40–50% higher expression levels of transcripts encoding microtubule-associated protein 1b (MAP1b), neurofilament heavy chain subunit (NEFH), A kinase anchor protein (AKAP), nestin (NES), Homer1 (HOMER1), and activity-regulated cytoskeletal-associated protein (ARC). Levels of these transcripts were not significantly different between the baseline and IVIG group. **B**) Six months of IVIG resulted in ~50% higher levels of NEFH, AKAP, NES, and ARC compared to placebo. Levels of these transcripts were not significantly different between the baseline and IVIG group. $n = 12$/group *, $p < 0.01$, **, $p < 0.001$ via one-way ANOVA with Bonferroni's *post hoc* test for multiple comparisons. Other abbreviations: ACTB (β-actin), TUBB2C (β-tubulin), MAP2 (microtubule-associated protein 2), NFEL and NFEM (neurofilament light and medium chain subunits), UTRN (utrophin).

Author Manuscript Author Manuscript Author Manuscript Author Manuscript

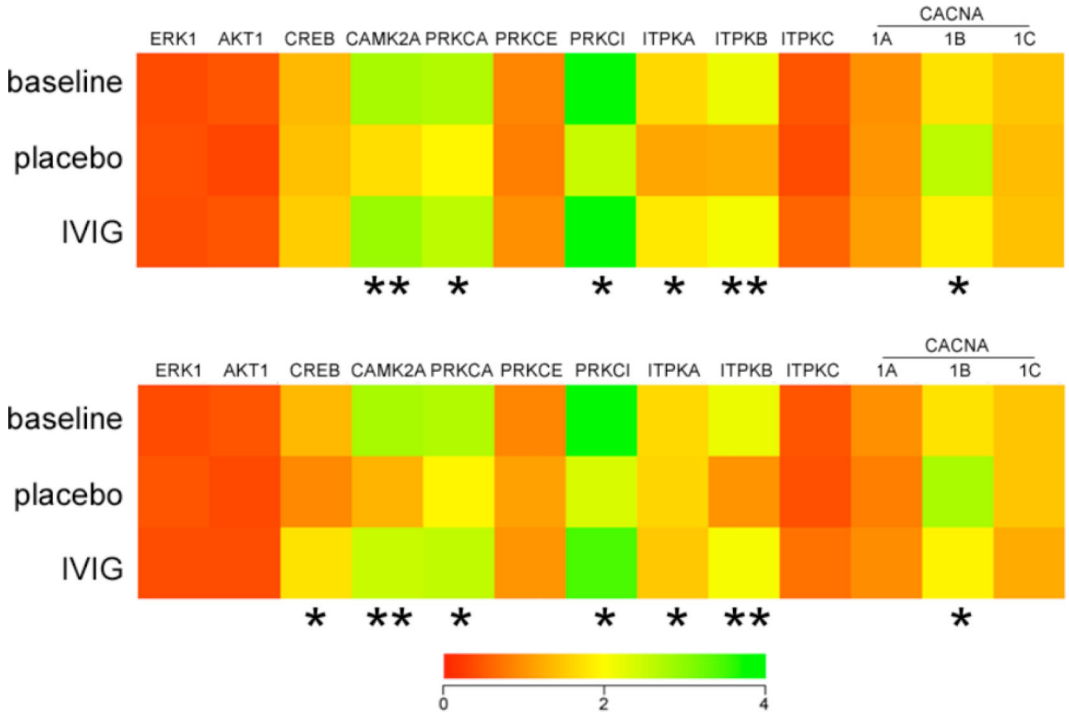

Fig. (6).

IVIG regulates plasma levels of mRNAs encoding calcium-signaling molecules. Three months of IVIG altered plasma levels of select mRNAs regulating calcium-dependent intracellular signaling, synaptic plasticity, and cell survival. **A**) Heat map (red to green = increasing mRNA levels) shows that, compared to placebo, IVIG treatment resulted in 35–45% higher plasma levels of transcripts encoding calcium/calmodulin-mediated protein kinase 2A (CAMK2A), protein kinase C, alpha (PRKCA), protein kinase C, iota (PRKCI), and inositol triphosphate kinases A and B (ITPKA and ITPKB). By contrast, mRNA levels of voltage-gated calcium channel, N-type (CACNA1B) were decreased 35% with IVIG compared to placebo. Levels of these transcripts were not significantly different between the baseline and IVIG groups. **B**) Six months of IVIG resulted in ~50% higher levels of CAMK2A, PRKCA, PRKCI, ITPKA, and ITPKB. CREB transcripts levels were also increased 30% compared to placebo. Plasma CACNA1B levels were decreased 40% with IVIG compared to placebo. Levels of these transcripts were not significantly different between the baseline and IVIG groups. $n = 12$/group; *, $p < 0.01$, **, $p < 0.001$ via one-way ANOVA with Bonferroni's *post hoc* test for multiple comparisons. Other abbreviations: (ERK1 (extracellular signal related kinase 1), AKT1 (v-akt viral oncogene homolog 1), CREB (cAMP-response element binding protein), PRKCE (protein kinase C, epsilon), ITPKC (inositol triphosphate kinase C), CACNA1A (voltage-gated calcium channel, P/Q-type), CACNA1C (voltage-gated calcium channel, L-type).

Author Manuscript Author Manuscript Author Manuscript Author Manuscript

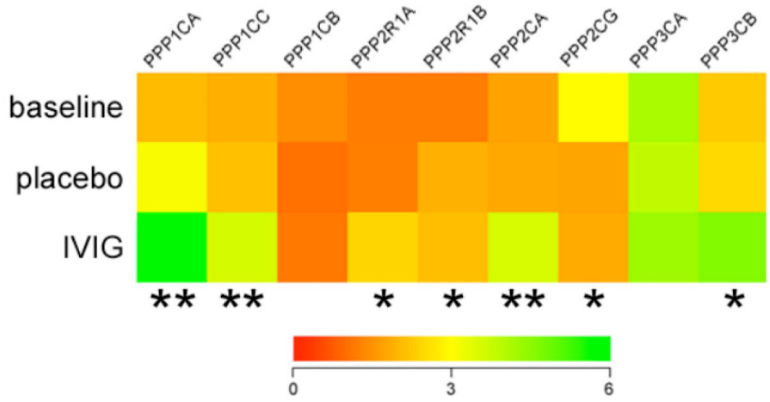

Fig. (7). IVIG regulates plasma levels of mRNAs encoding protein phosphatase subunits.

Heat map (red to green = increasing mRNA levels) shows that, compared to placebo, six months of IVIG treatment resulted in 40–50% increases in protein phosphatase 1, catalytic subunit, alpha isozyme (PPP1CA); protein phosphatase 1, catalytic subunit, gamma isozyme (PPP1CG); protein phosphatase 2, regulatory subunit A, alpha (PPP2R1A); protein phosphatase 2, catalytic subunit, alpha isozyme (PPP2CA); and protein phosphatase 3, catalytic subunit, beta isozyme (PPP3CB). Levels of these transcripts were not significantly different between the baseline and IVIG groups. By contrast, levels of protein phosphatase 2, regulatory subunit A, beta (PPP2R1B), were increased ~40% in both placebo and IVIG groups compared to baseline, whereas levels of protein phosphatase 2, catalytic subunit, gamma isozyme (PPP2CG), were reduced ~60% % in both placebo and IVIG groups compared to baseline. $n = 12$/group; *, $p < 0.01$, **, $p < 0.001$ via one-way ANOVA with Bonferroni's *post hoc* test for multiple comparisons. Other abbreviations: PPP1CB (protein phosphatase 1, catalytic subunit, gamma isozyme), PPP3CA (protein phosphatase 3, catalytic subunit, alpha isozyme).